ANTIOXIDANTS & REDOX SIGNALING
Volume 15, Number 5, 2011
© Mary Ann Liebert, Inc.
DOI: 10.1089/ars.2010.3365

FORUM REVIEW ARTICLE

Animal, *In Vitro*, and *Ex Vivo* Models of Flow-Dependent Atherosclerosis: Role of Oxidative Stress

Amir Rezvan,[1] Chih-Wen Ni,[2] Noah Alberts-Grill,[1] and Hanjoong Jo[1–3]

Abstract

Atherosclerosis is an inflammatory disease preferentially occurring in curved or branched arterial regions, whereas straight parts of the arteries are protected, suggesting a close relationship between flow and atherosclerosis. However, evidence directly linking disturbed flow to atherogenesis is just emerging, thanks to the recent development of suitable animal models. In this article, we review the status of various animal, *in vitro*, and *ex vivo* models that have been used to study flow-dependent vascular biology and atherosclerosis. For animal models, naturally flow-disturbed regions such as branched or curved arterial regions as well as surgically created models, including arterio-venous fistulas, vascular grafts, perivascular cuffs, and complete, incomplete, or partial ligation of arteries, are used. Although *in vivo* models provide the environment needed to mimic the complex pathophysiological processes, *in vitro* models provide simple conditions that allow the study of isolated factors. Typical *in vitro* models use cultured endothelial cells exposed to various flow conditions, using devices such as cone-and-plate and parallel-plate chambers. *Ex vivo* models using isolated vessels have been used to bridge the gap between complex *in vivo* models and simple *in vitro* systems. Here, we review these flow models in the context of the role of oxidative stress in flow-dependent inflammation, a critical proatherogenic step, and atherosclerosis. *Antioxid. Redox Signal*. 15, 1433–1448.

Introduction

The relationship between atherogenesis and blood flow or arterial wall shear stress has been studied for over 40 years (16, 17, 28, 33, 37, 47, 55, 64, 107, 170). Although some suspected that mechanical damage to the endothelium caused by suction forces (164) or high shear stress (47) was grounds for atherosclerosis, prevailing evidence supports that atherosclerosis is correlated to areas of flow separation (43, 64, 189), low shear stress (17, 18, 189), and oscillatory flow (89). The role of high shear stress re-emerged later in the context of plaque vulnerability (99). Apart from the magnitude and direction of shear stress, spatial (119) and temporal (4, 122, 180) gradients of shear stress are also important determinants of endothelial cell (EC) response. Moreover, a recent study from our group has shown direct evidence demonstrating that disturbed flow indeed leads to rapid development of atherosclerosis in a mouse model (121). In addition, this disturbed flow-induced atherosclerosis was mediated in part in an NADPH oxidase (Nox)-dependent manner (121). Here, we review these *in vivo*, *ex vivo*, and *in vitro* models in the context of studies designed to understand the role of oxidative stress in flow-mediated inflammation, a critical proatherogenic step, and atherosclerosis.

Animal Models of Atherosclerosis

Animal models play an essential role in helping us understand the pathophysiology of disease. Although no animal model is a perfect replica of the biological and pathophysiologic process in patients, they provide us with conditions that can be manipulated to clarify the process in such ways that would be impossible or unethical to perform in humans. Many of the animal models that will be discussed have been used effectively to demonstrate the important role of oxidative stress and nitric oxide (NO) signaling in atherosclerosis.

Many different animal species have been used as models for atherosclerosis (2, 69, 75). Different strains of the same species have varying susceptibility to atherosclerosis (75, 124). Some animals such as pigeons have naturally occurring lesions, whereas in others such as mice, an intervention such as genetic manipulation, special diet, or surgical intervention is needed to produce plaque. In many cases, interventions are used to accelerate plaque formation or alter the severity/complexity of the lesions.

[1]Division of Cardiology, Department of Medicine, Emory University, Atlanta, Georgia.
[2]Coulter Department of Biomedical Engineering, Georgia Institute of Technology and Emory University, Atlanta, Georgia.
[3]Department of Bioinspired Science, Ewha Womans University, Seoul, South Korea.

Larger animal models such as pigs, minipigs, and primates benefit from larger arterial size, and are therefore more relevant to human studies in addition to providing larger sample sizes of protein and RNA as well as opportunities for percutaneous interventions. The mouse has become one of the most important animal models (182) because of its numerous attributes such as relatively low cost, amenability to genetic modifications (knockout [KO] or transgenic mice), a completely mapped genome, availability of reagents (antibodies, siRNAs, microRNAs, *etc*.), and manifestation of cardiovascular diseases resembling at least some aspects of human pathophysiology.

Hypercholesterolemia-induced atherosclerosis

Although early attempts to cause atheromas in mice were unsuccessful, certain strains of mice do form atheromas in certain experimental models (124, 168). Many mouse models of atherosclerosis rely on inducing hypercholesterolemia by a combination of genetic mutation and high-fat diet. The most susceptible inbred mouse strain commonly used is the C57BL/6J strain. The susceptibility to atherosclerosis in different mouse strains does not correlate with the degree of hypercholesterolemia induced (124). In the past two decades, multiple genetic modifications have helped produce hyperlipidemic mice. Two of the most widely used genetic manipulations are disruption of the apolipoprotein E (ApoE) gene (127, 130, 193) and deficiency of the low-density lipoprotein receptor (70).

Many different custom diets are used in animal models to induce or accelerate atherosclerosis. There are two commonly used types of atherogenic diet in hyperlipidemic mouse models. Paigen's high-fat diet includes cholate and was originally made by mixing the Hartroft–Thomas diet (167) with a nonatherogenic diet (123). The Western diet contains no cholate and is considered less inflammatory and less potent in its atherogenic properties, but is also shown to be capable of promoting atherosclerosis in genetically deficient mice (100, 130).

Arterial injuries inducing atherosclerosis

Different models of arterial injury have been used, mostly as models of vascular remodeling and wound healing. Although in many of these models local shear stress is affected because of remodeling of the vessel in response to the injury, these are not regarded as models for flow-induced atherosclerosis.

An immunologic vascular injury by repeated injection of foreign proteins produced cellular lesions in larger arteries of rabbits fed an atherogenic diet (59, 110). A drying model of endothelial injury in rats (30) was used as the main arterial injury model in rodents until a wire injury model was established in the mouse (101) and followed later by balloon injury models (42, 115). The wire and balloon injury models are appropriate models to study restenosis in the context of vascular injury because of percutaneous interventions. Electrical injury stenosis (15) and chemical injury stenosis (82, 194) both induced from the adventitial side of blood vessels cause a transient thrombus formation and eventually lead to neointima formation.

The nonconstrictive perivascular cuff model initially used in rabbits (10) is another example of vascular injury induced from the adventitia leading to neointimal thickening, though in a more inflammation-based model. The role of possible local ischemia because of vasa vasorum occlusion was suggested in this model. The advantage of this model is that the vascular cells are not directly killed by an electric current or chemical. This model was the basis of constrictive perivascular cuff models that will be discussed below and was later modified for use in mice, resulting in accelerated atherosclerosis in a hyperlipidemic mouse model (61, 91, 145) and hyperlipidemic rabbits (183).

Animal models of flow-dependent atherosclerosis

Since atherosclerosis is a local disease, occurring mostly in areas of low and oscillatory shear (OS) stress—key features of disturbed flow—many have focused on studying the areas of naturally occurring disturbed flow in animal models, whereas others have attempted to create areas of disturbed flow to mimic the shear stress profile experienced in areas of naturally occurring atherosclerosis. Shear stress levels vary not only in different regions of the arterial tree within each species, but also considerably between different species, with higher shear stress values generally seen in smaller animals (22). Change in vessel diameter in response to shear stress alterations is not only species dependent but also strain dependent (68).

Areas of naturally occurring disturbed flow. For many years, atherosclerosis research in animal models was performed mostly by studying spontaneous atherosclerosis in animals susceptible to atheroma formation (75). In all the animal models discussed above, in which no surgical intervention is performed, atherosclerosis is predominantly seen in areas of disturbed flow. A disturbed pattern of flow can be found in many different areas of the arterial tree, including, but not limited to, the aortic root, lesser curvature of the aortic arch, root of the innominate artery, carotid bifurcation, branching of the celiac artery from the abdominal aorta as well as certain regions in the coronary system (3, 13, 26, 35, 41, 84, 93, 106, 161, 162). The predilection of these sites to atherogenesis is what brought the relationship of mechanical forces and atherosclerosis to the attention of investigators. Although these areas can be used to study the effects of disturbed flow on endothelial biology, including gene and protein expression, in many animals especially in mice, a hyperlipidemic model needs to be added to induce atherosclerosis in these regions.

The major advantage of using these areas of naturally occurring disturbed flow is the pathophysiologic relevance, as these are the areas that atheromas form in atheroprone species such as humans. These areas are chronically exposed to disturbed flow patterns. Therefore, although they are appropriate models for long-term atheroma formation, they are inadequate for assessing the effects of acute changes in shear stress. They may have adopted compensatory mechanisms to the disturbed flow pattern and other local conditions may also contribute to the disease. Another drawback is that in most of these models, the area exposed to disturbed flow is usually a very confined area. As such, the sample size for collecting protein and mRNA for analysis is very limited (181). Still, examining areas of naturally occurring disturbed flow is the oldest model used to look at the effects of shear stress on atherosclerosis and as such has produced the largest body of

information currently available in the field (29, 34, 76, 125). For example, these areas of naturally occurring disturbed flow were used to show that gp96^{phox} deficiency in phagocytes did not affect atherosclerosis formation (83) and that p47^{phox} is required for atherosclerotic lesion progression in ApoE KO mice (6). The ApoE KO on high-fat diet model was recently used to show the role of Nox2-mediated reactive oxygen species (ROS) production on atherosclerosis (78) as well as the protective role of dietary polyphenols on atherosclerosis (103).

Models inducing acute changes in shear stress. Although some interventions that likely changed flow patterns and shear stress were found to produce severe atherosclerosis—such as the coarctation of proximal aorta producing severe atherosclerosis in experimental dogs (143)—the specific role of acute changes in shear stress was not assessed until the 1980s. The initial models were used to show the effect of shear stress on vascular diameter by creating an arterio-venous (A/V) shunt (79, 190), placing a restrictive clip around the artery (56), or changing the viscosity of blood (109) as well as showing the effect of shear stress on EC morphology *in vivo* (95). Importantly, this model was used to demonstrate that the change in vascular diameter in response to shear stress is dependent on intact vascular endothelium (90).

With technological advances and development of faster computers and more powerful software, the accuracy in calculation of shear stress in the arterial tree has increased significantly in the past few decades. More recently, finite element modeling and computational fluid dynamic methods have allowed investigators to assess wall shear stress more accurately in complicated and realistic situations of pulsatile flow conditions and curving and branching vessels (20, 65, 66, 121, 133, 136, 160, 161, 188).

A/V fistula. One of the first models to incorporate an intervention causing acute change in shear stress is the A/V fistula (190). In this model blood flow is increased in the artery from which the fistula is created. It was shown that in response to the increased shear stress, the lumen of the artery dilates to the extent that the final shear stress is not significantly different from the original shear stress. In humans, the effect of increased shear stress on vascular remodeling caused by A/V fistula has been shown in chronic kidney disease patients who undergo A/V fistula formation for the purpose of dialysis access (50). This model was used to show the regulatory role of p47^{phox} component of Nox on shear stress-induced vascular remodeling (19).

Vascular grafts. The use of vein grafts as a model for atherosclerosis was originally developed to study the pathophysiology of atherosclerosis in coronary artery bypass graft patients. The saphenous vein graft is widely used for the purpose of coronary artery bypass. However, it is now well known that the occlusion rate in these venous grafts is much higher than when using an arterial graft such as the internal mammary artery. To better understand the pathogenesis of venous graft occlusions, animal models of venous grafts have been used (38, 40, 58, 63, 98, 150, 195). This method involves end-to-end transplantation of the inferior vena cava or external jugular veins to the common carotid artery (Fig. 1). Although the fluid dynamics involved in this model have not been extensively studied, one can speculate that because of the larger diameter of the engrafted vein compared to that of the common carotid, lower shear stress is achieved in the engrafted vein compared with the contralateral artery, which is usually used as a control. Although this lower shear stress may be a contributing factor to atherogenesis in this model, owing to significant inherent differences between venous and arterial vessels, the relative contribution of change in shear stress will be very difficult to determine. This model has been modified as a chimeric model using human coronary artery grafts in mice (178). It also has the potential to allow the investigator to use a graft from a specific KO animal and create a model in which the investigator can effectively study the local KO effect of a certain gene in the process of atherosclerosis or vascular remodeling.

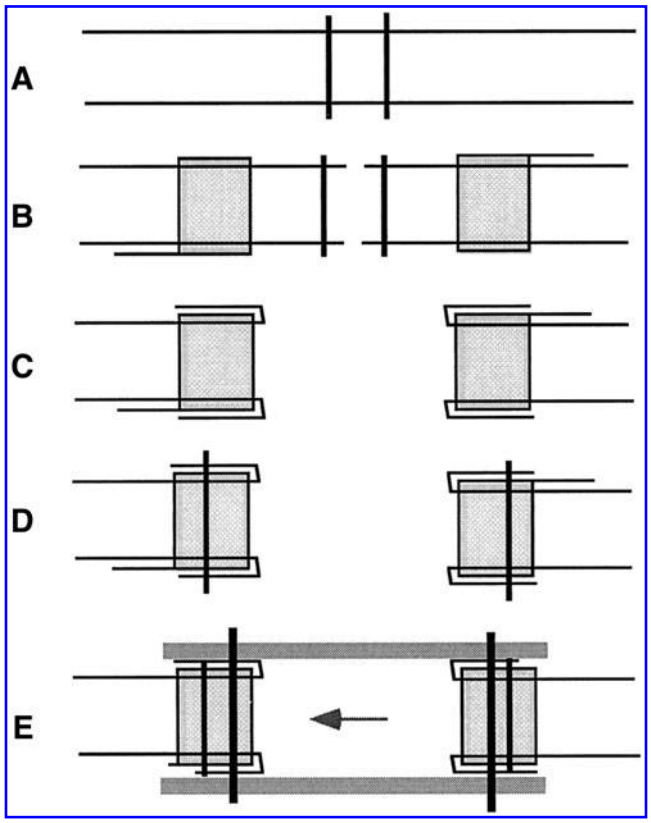

FIG. 1. Schematic representation of vein bypass graft in the common carotid artery. The right common carotid artery (RCA) was ligated with an 8-0 silk suture **(A)** and dissected between the middle ties and passed through the cuffs **(B)**. The suture at the end of the artery was removed, and a segment of the artery was turned inside out to cover the cuff body **(C)**, which was fixed to the cuff with an 8-0 silk suture **(D)**. The right external jugular or vena cava vein segment was harvested and grafted between the two ends of the carotid artery by sleeving the ends of the vein over the artery cuff and suturing them **(E)**. *Arrow* indicates direction of blood flow. The cuff handle was cut off, and the vascular clamps were removed. Reprinted with permission from Zou *et al.* (195).

Constrictive perivascular cuff. The perivascular cuff model was modified to a constrictive cuff used in hyperlipidemic animals to induce rapid atherosclerosis (23–25, 131, 132, 176, 177). In this model, while the vessel region constricted by the

cuff is exposed to higher shear stress, a proximal section of the post-constriction area is exposed to disturbed flow giving rise to low and OS stress patterns. An example of a recent such device that also incorporates a tapered lumen providing different levels of shear stress within the cuff is shown in Figure 2. This model has the ability to produce distinct flow patterns in neighboring regions. A drawback of this model is the requirement for direct manipulation of the vessel adventitia that may resemble the injury effect seen in the nonconstrictive perivascular cuff model. This model has been used to show the role of shear stress on endothelial NO synthase (eNOS) localization (25).

Ligations: complete, incomplete, and partial

Incomplete ligation. The incomplete ligation of an artery to assess the effect of shear stress on atherosclerosis was first used in Yucatan micropigs (148). By causing a 50% aortic stenosis, the authors showed that increased shear stress had a protective role against plaque formation in a hyperlipidemic model. More recently, a modified version of this model with 80% stenosis was used to show features of vulnerable plaque (71, 153).

Complete ligation. Complete ligation of the carotid artery has been widely used in rodents and causes vascular remodeling, neointimal hyperplasia (39, 53, 88, 108, 112, 115, 126, 134, 138, 156, 184, 191), and used to demonstrate the role of NO and ROS in this remodeling (80, 88, 102, 105, 115, 117, 139, 146, 185, 187) as well as atheroma formation when used in hyperlipidemic animal models (31, 72, 77, 81, 94, 102, 120, 139, 145, 174, 183, 192). The complete ligation model leads to abrupt cessation of blood flow, essentially reducing wall shear stress to zero and therefore can be accounted as a shear stress modifying model. However, because of thrombus formation and significant endothelial injury as well as the low relevance of no-flow conditions to atheroma formation in humans, it may not be a suitable model to study the effects of shear stress in atherosclerosis and is better viewed as a model of arterial injury.

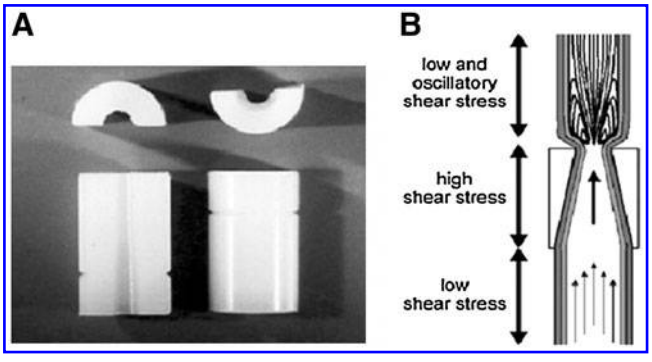

FIG. 2. Perivascular cuff model and its shear stress patterns. (A) The cast consists of two longitudinal halves of a cylinder with a conical lumen. **(B)** The theoretical design with induction of large vortices downstream of the cast in the carotid artery. Additionally, the conical lumen induces a stenosis of the vessel, causing a gradual increase in vascular shear stress in the cast area. A region of low shear stress is created upstream of the cast. Reprinted with permission from Cheng *et al*. (25).

Partial ligation model. The complete ligation model has evolved into a modified partial ligation model of the carotid artery (85, 86, 111, 141, 142, 159, 163) that was shown to cause reduced flow in the ligated artery and shear stress-dependent vascular remodeling of the carotid artery in mice in an NO/ROS-dependent manner. We recently characterized this model further and showed that by ligating the internal carotid, the occipital, and the external carotid after the branching of the superior thyroid artery, allowing common carotid blood flow only through the superior thyroid artery (Fig. 3), not only is the flow rate significantly reduced, but also a flow reversal pattern is seen during diastole, giving rise to a combined low and OS stress pattern that is characteristic of areas of disturbed flow in the arterial tree (121).

With this model and a high-fat diet feeding, we have directly demonstrated that acutely imposed disturbed flow induces robust atherosclerosis by 2 weeks and complex lesion formation by 4 weeks after partial ligation in the common carotid of ApoE KO mice (121). We have also shown that disturbed flow alters EC gene expression and $p47^{phox}$-dependent ROS formation within 2 days and endothelial dysfunction within 7 days (121). Moreover, we used this model to test the role of ROS in flow-induced atherosclerosis by comparing ApoE-null mice and $p47^{phox}$_ApoE double KO mice. We found that disturbed flow increased superoxide production in ApoE KO mice that was significantly blunted in $p47^{phox}$_ApoE double KO mice. We also found that flow-induced atherosclerosis in $p47^{phox}$_ApoE double KO was significantly less in the early phase (2 weeks postsurgery) than ApoE KO, but this difference began to disappear by 3 weeks postsurgery (121).

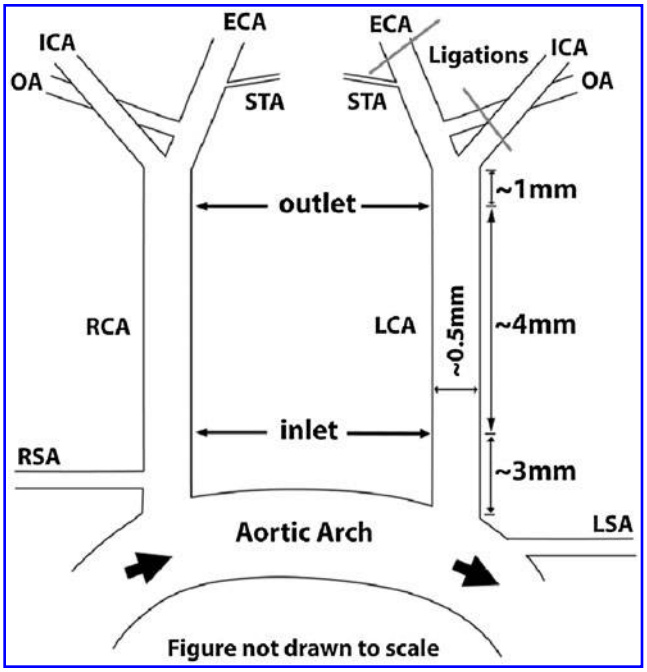

FIG. 3. Schematic of partial ligation of the left common carotid artery (LCA) branches. Three branches of the LCA (external carotid artery [ECA], internal carotid artery [ICA], and occipital artery [OA]) were ligated using 6-0 suture, while leaving the superior thyroid artery (STA) patent to create oscillatory and low shear stress in the LCA. Reprinted with permission from Nam *et al*. (121). LSA, left subclavian artery; RSA, right subclavian artery.

These results suggest that $p47^{phox}$-dependent ROS plays a critical role in early atheroma formation, but ROS produced from other sources become more important in the late phase of the disease. The alternative sources of ROS are not known yet, but mitochondria and uncoupled eNOS are some of the potential candidates. Using this model, we have also shown that low and OS is associated with impaired GTP cyclohydrolase-1 phosphorylation and reduced tetrahydrobiopterin levels *in vivo* (97). In this model, the left common carotid artery, where atheroma develops, is un-touched or not manipulated during the partial ligation surgery to minimize direct injury to the common carotid. In fact, performing sham partial ligations, including performing the surgery and tying loose knots around the branches of the common carotid artery, does not result in atheroma formation within the timeframe studied. An additional advantage of this model is the availability of the large portion of the carotid arteries that allows easy and reproducible intimal RNA isolation, enabling RNA studies such as qPCR and genome-wide analysis of cDNA and microRNA to identify mechanosensitive transcripts and pathways.

In Vitro Models for Shear Stress Studies

To investigate how local hemodynamic conditions regulate EC function *in vivo*, several *in vitro* systems have been developed (140). Devices such as the parallel-plate flow chamber, vertical step flow chamber, cone-and-plate viscometer, modified cone-and-plate shear apparatus, and microfluidics devices have allowed for controlled experiments on cultured ECs (27, 32, 60, 140, 158). The cone-and-plate and parallel-plate flow chamber are two of the most popular *in vitro* shear devices. Here, we will discuss prototypes of each model.

Cone and plate

The first well-characterized *in vitro* shear stress device was introduced by three pioneers of endothelial mechanobiology—Forbes Dewey, Peter Davies, and Michael Gimbrone—using the geometry of a cone-and-plate viscometer (14, 36). In this system, shear stress is produced by rotating a cone over a stationary plate containing ECs cultured on cover slips. Using this device, it was demonstrated for the first time that shear stress can regulate EC shape and orientation as well as more complex biological functions such as wound regeneration, fluid endocytosis, and platelet/endothelium interactions. Although this original cone-and-plate or viscometer system has since been modified by numerous groups, including us, it ushered a new field of endothelial mechanobiology.

A modified cone-and-plate design was published in 1984 by Franke *et al.* (46, 151). The authors fitted a transparent polycarbonate cone into a Plexiglas holder and connected the cone to a speed-controlled motor with variable rotational velocities. The entire cone-and-plate system was connected to an optical system, which allowed direct observation in a real-time manner in response to shear stress. In this study, the results clearly showed that endothelial stress fibers can be induced by a 3-h exposure of ECs to fluid shear stress of 2 dyn/cm^2, suggesting that shear stress may act directly on the stress fiber system without affecting cellular shape and orientation.

The disadvantages of the cone-and-plate devices have been addressed recently (8, 9, 155). Blackman *et al*. developed a new controlled cell shearing device (Fig. 4) based on the cone-and-plate viscometer that utilized a microstepper motor technology to independently control the dynamic and steady components of the hydrodynamic shear–stress environment (8). This system also integrated a fluorescence microscopy system to allow real-time monitoring of cellular responses. These devices have been used to reproduce atherogenic or atheroprotective flow wave forms acquired *in vivo*, allowing the observation of endothelial responses to disease-relevant shear conditions (1, 32). Although this is a state-of-the-art device, a major disadvantage is the relatively high cost of custom manufacturing the system and culture dishes.

Tarbell and colleagues modified the cone-and-plate system to measure water flux across endothelial monolayer under shear stress (154). On the basis of a cone-and-plate apparatus, the luminal compartment contained a cylindrical disk, which was rotated by a drive motor assembly to produce a defined shear stress on the endothelial monolayer. With this special design they demonstrated that shear stress increases hydraulic conductivity of cultured endothelial monolayer through a cellular mechanism involving signal transduction.

Our lab has also developed a modified cone-and-plate shear apparatus (51, 74) (Fig. 5). The entire shear system except for the personal computer controller unit was housed in a humidified tissue culture incubator (5% CO_2, 37°C). The cone was rotated either back and forth or unidirectionally through an in-house computer program and a stepping motor to generate oscillatory and laminar shear (LS) patterns, respectively, or to mimic *in vivo* flow profiles. The shear system was designed to be used with a 10 cm tissue culture dish (Falcon)

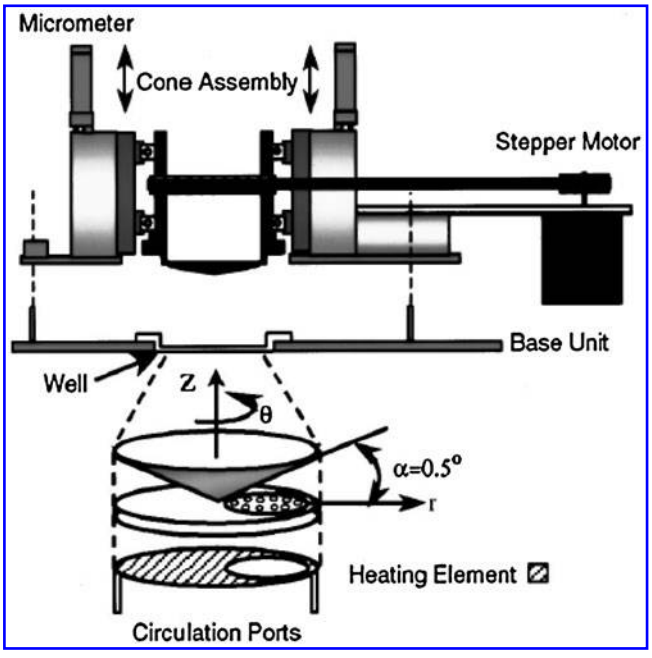

FIG. 4. Schematic of the controlled cell shearing device. The schematic shows the dynamic two degrees-of-freedom cone assembly, *z*-axis translation *via* dual micrometers, and rotation *via* microstepper motor. Reprinted with permission from Blackman *et al*. (8).

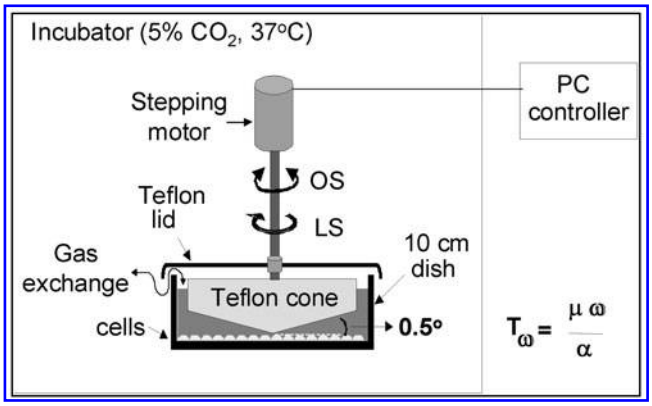

FIG. 5. Cone-and-plate shear device. Shown is a schematic of the modified cone-and-plate shear apparatus. The cone has a fixed 0.5° angle and is machined out of Teflon block. The entire shear system except for the computer controller unit is housed in a humidified tissue culture incubator (5% CO_2, 37°C). The cone is rotated back and forth or unidirectionally through an in-house computer program and a stepping motor to generate oscillatory shear (OS) and laminar shear (LS), respectively, or to mimic *in vivo* flow profiles. Reprinted with permission from Jo *et al*. (73).

and the Teflon lid was designed to allow free gas exchange between the cells and the incubator environment, while preventing contamination. We have used this system to identify several shear sensitive genes and their biological function. For example, we have shown that OS stress induces expression of bone morphogenetic protein 4 (BMP4), angiopoietin 2, peroxiredoxin, and cathepsins L and K, and investigated their roles in inflammation, vasculogenesis, vascular remodeling, and oxidative stress (21, 116, 128, 129, 157, 158, 171). The advantages of this modified system are that it is extremely simple to use (just put a cone to a standard 10 cm culture dish), and is well suited for chronic studies (hours to days) with virtually no threat of contamination because the cone is housed in a lid unit that sits on the dish. The system also provides large quantities of protein and RNA from single 10 cm dishes. However, there are some disadvantages to using this type of device. For example, EC monolayers are not subjected to uniform shear stress levels as a shear–stress gradient is produced from the center toward the edge of the dish. In addition, our system has a smaller cell-to-volume ratio and does not permit continuous sampling of the cell culture medium. It also permits the culture medium to evaporate, which requires replenishing with fresh medium and is not set up to allow us to monitor cell behavior in real time.

Using our cone-and-plate shear device, we have shown that exposure of ECs to OS stimulates ROS production from Noxs, which in turn results in monocyte adhesion (157). Hwang *et al.* have shown that OS increases Nox2 and Nox4 mRNA level after 4 and 8 h of exposure (67, 157). Similarly, our group has shown that Nox1 and Nox2 were increased after 24-h exposure to OS stress (67). These findings prompted the question of whether BMP4 produced in ECs by OS is directly responsible for production of ROS from Noxs, which then leads to inter-cellular adhesion molecule 1 (ICAM-1) induction and monocyte binding. Our initial studies using pharmacological approaches *via* ROS scavengers such as N-acetyl-cysteine, the cell-permeable polyethylene glycol-catalase, polyethylene glycol-superoxide dismutase, and Tiron completely blocked OS- and BMP4-induced monocyte binding and ICAM-1 expression, demonstrating a role for ROS in these processes (67, 157). Further, we showed that mouse aortic ECs obtained from Nox KO mice lacking $p47^{phox}$ (MAE-$p47^{-/-}$ cells) (67) did not produce ROS in response to OS or BMP4. ROS production in these cells was rescued by transfecting them with $p47^{phox}$ cDNA. A similar approach was used in MAE-$p47^{-/-}$ cells to demonstrate that OS and BMP4 stimulate monocyte adhesion by a mechanism dependent on ROS derived from $p47^{phox}$-based Noxs (157). These findings suggest that exposure of ECs to OS induces BMP4 production, which in turn triggers proinflammatory and proatherogenic responses of ECs by increasing ROS production from Noxs.

Parallel-plate flow chamber

Frangos, McIntire, and colleagues (44, 45) developed a parallel-plate flow chamber, which has been widely used and modified by many groups (87, 92, 96). The design of the flow chamber consists of a machine-milled polycarbonate plate, a rectangular Silastic gasket, and a glass slide (or cover slip) with the attached EC monolayer (Fig. 6). These were held together by a vacuum maintained at the periphery of the slide, forming a channel of parallel-plate geometry. Flow was driven either by the hydrostatic pressure head between the two reservoirs to produce steady flow or *via* cam-driven clamps upstream of the chamber to produce pulsatile flow.

Parallel-plate flow chamber devices have been used to document changes in EC morphology (96) and metabolism (44, 45) in response to shear stress, as well as to successfully model leukocyte–endothelium adhesion interactions under flow conditions (92). Thereafter, several modified designs have been used to investigate many important topics. For example, to study the effects of shear on EC monolayer permeability, we attached the flow chamber to a circulating luminal perfusion loop and a noncirculating abluminal loop (73). Usami *et al.* published a modified parallel-plate system in 1993 that used a flow chamber with a center arrow-shaped channel capable of generating variable shear stresses within the same flow field without changing the flow rate or gap width because of the geometry of the channel (175). This design could generate a variable shear stress, because of the geometry of the channel, within the same flow field without changing the flow rate or the gap width, starting from a predetermined maximum value at the entrance and falling to zero at the exit. Studies conducted using this device demonstated that expression of adhesion molecules such as vascular cell adhesion molecule 1 (VCAM-1) and E-selectin was suppressed proportional to increased shear stress in cultured human aortic ECs (173). Also, this gradient flow chamber has been used to study the effects of different shear rates on platelet adhesion onto immobilized fibrinogen and von Willebrand factor matrices (147).

Flow characteristics such as flow separation, recirculation, and reattachment in areas such as arterial bifurcations may directly contribute to the initiation of focal atherogenesis. Spatial and temporal gradients in shear stress overlap in atherosclerosis prone regions, and a specially designed flow device was needed to separate these two factors to determine their effects on atherosclerotic plaque growth. The sudden expansion flow chamber (172) and the backward-facing step flow chamber (57) were developed to create the separated

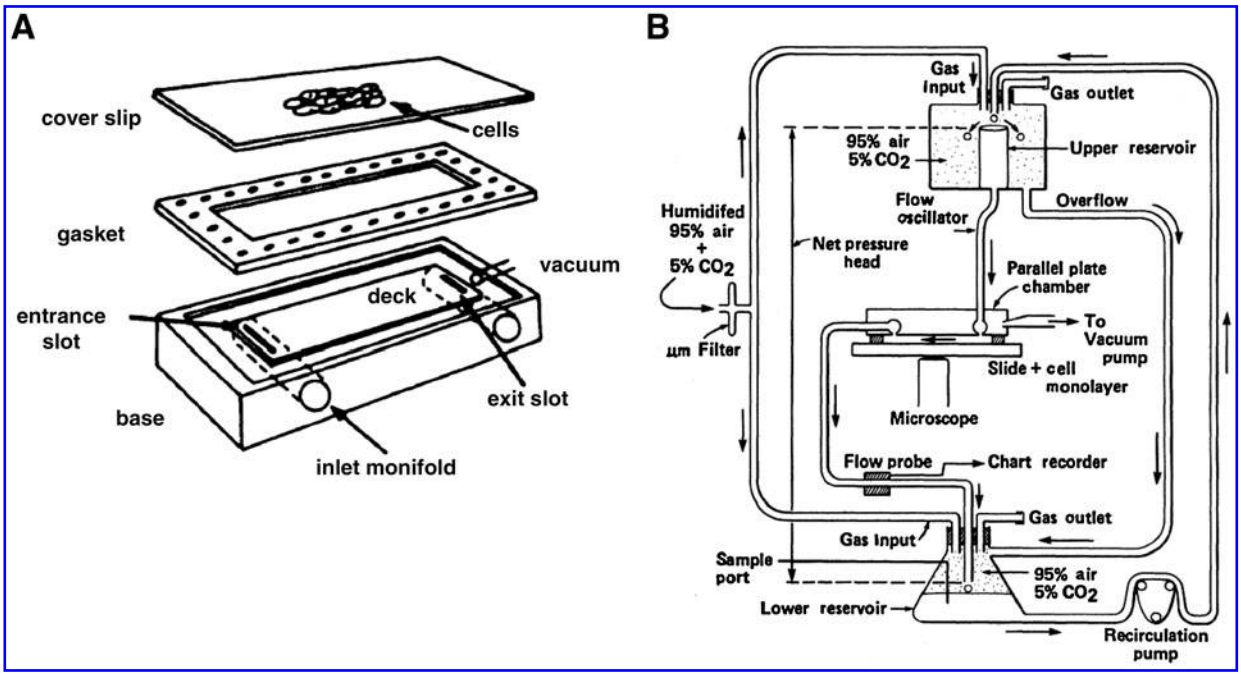

FIG. 6. Parallel-plate flow chamber and schematic diagram of flow loop. (A) Parallel-plate flow chamber. The polycarbonate plate, the gasket, and the glass slide with the attached cells are held together by a vacuum, forming a channel of parallel-plate geometry. Medium enters at entry port, through slit, into the channel, and exits through slit, and exit port. Reprinted with permission from Lawrence *et al.* (92). **(B)** Drawing of flow loop. Reprinted with permission from Frangos *et al.* (44).

flow streams by which ECs experience large spatial shear stress gradients. In the sudden expansion model, fluid flows from a narrow channel over a step expansion into a wider channel. The asymmetric expansion of the flow path leads to flow separation. Close to the expansion step, there is a recirculating eddy with a flow direction against the main flow. Farther downstream, the flow reattaches and eventually reestablishes a unidirectional parabolic flow profile. In addition, the temporal gradient in the step flow chamber can be effectively eliminated by changing the rate of flow onset. In experiments on ECs, disturbed flow stimulated cell proliferation only when flow onset was sudden, and the spatial patterns of proliferation rate match the exposure to temporal gradients (57). A different design of flow system by Hsiai *et al.* was used to study the effect of various upstroke slopes of pulsatile flow, also known as shear stress slew rates (62). The inlet and outlet of a parallel channel was connected to symmetrical contractions and diffusers ensuring uniform velocity and preventing flow separation across the channel. This flow system was able to precisely control the frequency, amplitude, and time-averaged shear stress of pulsatile flow and allowed the investigators to study the effect of slew rates independent from other factors. Using this system, it was observed that EC remodeling was faster in response to higher slew rates at a given time-averaged shear stress.

The parallel-plate flow chamber is widely used by numerous groups with various modifications; however, setting up a flow system may not be easy for scientists without engineering background. As such, several commercially designed flow systems based on the parallel-flow chamber are available (GlycoTech, Flexcell, *etc*.). Brown and Larson compared the original and commercially designed (GlycoTech) flow chambers and concluded that the chamber from GlycoTech dramatically reduced reagents use and cell requirements and could be useful in a variety of shear experiments (12)

Coculture shear stress system: a modified parallel-plate system

Since the vessel wall is composed of several types of cells, including ECs, smooth muscle cells (SMCs), and fibroblasts, heterogenous cell–cell interactions could govern numerous biological events in both healthy and diseased vasculature. Coculture models place ECs in proximity to SMCs to better simulate the *in vivo* environment. Nackman *et al.* first developed a parallel-plate flow chamber into which a coculture permeable membrane is inserted (Fig. 7). In this model, ECs were cultured on one side of the membrane and exposed to laminar flow, whereas SMCs were cultured on the other side of the membrane and not directly exposed to flow (118). Using this system, they exposed the EC side of the coculture to low shear stress and showed that the proliferation of the neighboring SMCs was attenuated (118). Rainger *et al.* and Chiu *et al.* also established similar parallel-plate coculture systems (27, 137). It was shown that coculture of ECs with SMCs markedly increased the adhesion of flowing leukocytes to ECs (137). Further, LS stress inhibited expression of adhesion molecules such as ICAM-1, VCAM-1, and E-selectin in ECs induced by coculture with SMCs (27), suggesting that SMCs may induce inflammatory responses in ECs and LS stress acts as a protective regulator of atherogenesis (152).

Microfluidic devices

The cone-and-plate and parallel-plate flow chamber are the most wildly used systems in shear stress studies. However, these gold standard systems are not suitable for certain types

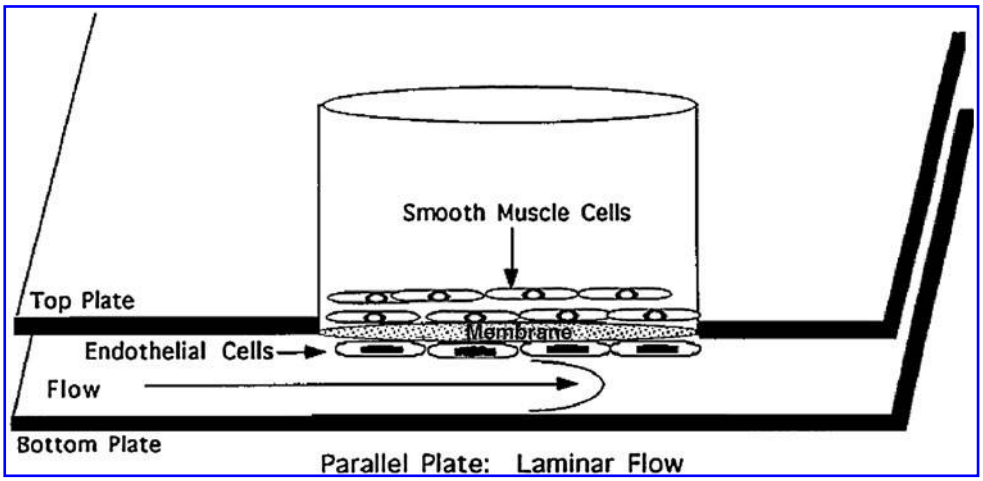

FIG. 7. Schematic diagram of coculture apparatus inserted into aperture of parallel-plate flow device. Reprinted with permission from Nackman *et al.* (118).

of research such as high-throughput screening studies because of the large number of ECs needed and the large volumes of culture medium and reagents needed to maintain them. To address these issues, Schaff *et al.* have developed the vascular mimetic microfluidic chamber, which is designed to precisely control the input concentration of cells and reagents over time and to observe the leukocyte–EC interactions in real time (Fig. 8A) (149). Using this device, the authors examined the relationship between hydrodynamics and neutrophil recruitment. Another microfluidics system was designed to study the effects of shear stress on platelet adhesion (54). Gutierrez *et al.* demonstrated that the microfluidic devices made of polydimethylsiloxane (PDMS) sealed with a cover glass could be used to study dynamic platelet adhesion with volume requirements reduced to less than 100 μl per assay. In addition, the PDMS microfluidic device has also been further modified with a magnetic clamp to seal PDMS chips against cover glasses with cell cultures (169). It provides a reliable way for sealing microfluidic devices with little effect on the shear stress at the glass substrate during the perfusion. Moreover, microfluidic devices have been designed to study the responses of ECs exposed to pulsatile and OS stress in an integrated microfluidic chip with a pneumatic micropump (Fig. 8B) (152). These microfluidic devices show a great potential as a tool for an *in vitro* shear stress model with several benefits, including higher-throughput and reduced reagent use.

Other in vitro *systems*

Samet and Lelkes developed a pulsatile flow chamber model of an artificial cardiac ventricle device and studied EC morphology as well as gene expression patterns in response to disturbed flow conditions (11, 144). Another *in vitro* shear device that merits mention is a chamber device in which ECs cultured on a filter membrane in a chamber can be exposed to shear stress, an oxygen concentration gradient, and low-density lipoprotein loading. Using this system, Warabi *et al.* have shown the dominant role of shear stress in gene expression patterns in an Nrf2-dependent manner (179).

Simultaneous shear and strain device

Although shear stress is well studied and considered to be an important factor in vascular biology, circumferential strain driven by the pulsing wall motion also showed significant effects on endothelial biology (7). The interaction of shear stress and strain may influence the responses of ECs, and a specific design of flow system has been designed to investigate EC biological responses to simultaneous OS stress and strain over a physiological range of stress phase angle (SPA) (114, 135). ECs were cultured on the inside walls of elastic, silicon rubber tubes, and a pulsatile flow loop was developed

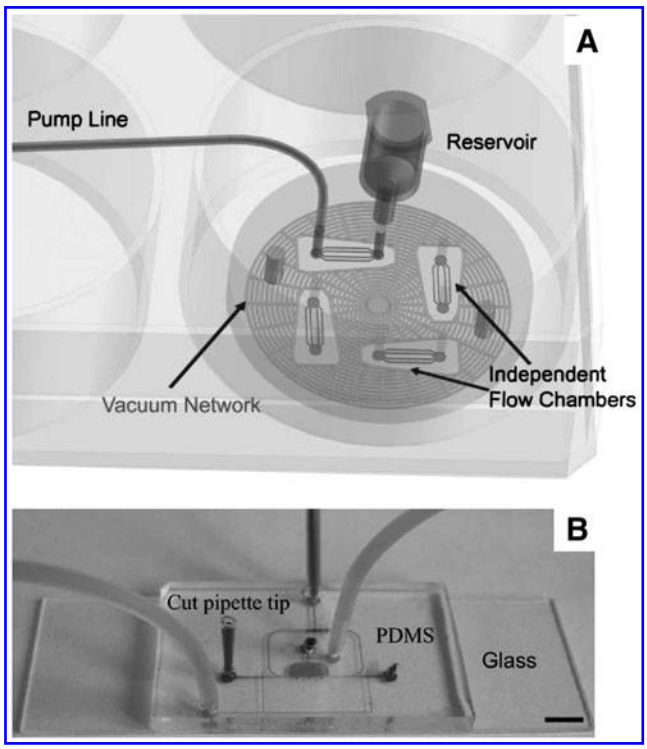

FIG. 8. Microfluidic devices used to study the effects of shear stress on endothelial cells. (A) Schematic of the vascular mimetic device. The silicon master pattern produces a flow chamber consisting of four independently operated sets of channels, which are isolated by intervening vacuum lines. Reprinted with permission from Schaff *et al.* (149). **(B)** Schematic illustration of the microcirculatory system on the chip. A top view of the chip with tubings connected and a cut pipette tip inserted (filled with dye for observation). Reprinted with permission from Shao *et al.* (152).

to generate OS stress and circumferential strain. The results of this study showed that strain tends to enhance the vasodilatory tendency, and this is modulated by the SPA (135), and it seems that the interaction of shear stress and strain can also influence vascular remodeling. Thus, this model could be used to further study multiple mechanical stimuli with different SPA and help to elucidate the detailed mechanisms.

Ex Vivo Organ Culture Models

In vitro models obviously provide a gold standard of experimental control, but fail to replicate the complex cell–cell and cell–matrix interactions that occur *in vivo* and likely play a central role in the relationship of oxidative stress, shear stress, and atherosclerosis. To account for this, *ex vivo* organ culture models have been to bridge the gap between *in vitro* and *in vivo* research on the relationship between shear stress and oxidative stress.

History and background

Ex vivo models of sufficient sophistication and physiological relevance to replicate *in vivo* conditions of pressure, shear, and stretch have existed since the early 1990s. In these models, explanted artery segments are canulated at either end in a culture medium bath and plugged into a perfusion circuit to allow perfusion of the arterial segment with directional fluid flow. Closed-circuit perfusion systems exist that provide control of intraluminal pressure and flow pulsatility and direction in a sterile environment with the potential for long-term organ culture studies (5, 48).

Ex vivo *models of shear-induced oxidative stress*

Ex vivo models have been used by researchers in the atherosclerosis field to elucidate vascular wall responses to a number of physiologic mechanical forces and other biological processes thought to be involved in atherogenesis (186). Some of these studies focused on the relationship between shear stress and oxidative stress. Gambillara *et al.* showed that plaque-prone hemodynamics such as low and especially OS stress reduced eNOS expression in explanted *ex vivo* cultured porcine carotid arteries (48). Disturbed flow also impaired endothelial function by making exposed endothelium nonresponsive to bradykinin treatment. eNOS is important in oxidative stress and atherosclerosis for producing NO, which functions as a vasodilator and atheroprotective factor. As shown by Lu and Kassab, NO levels in *ex vivo* cultured porcine arteries sharply drop after exposure to reverse flow because of shear-induced production of superoxide by ECs (104). This effect was inhibited by adding a cell-permeable free radical scavenger such as tempol. Further work has tied shear-dependent increases in superoxide production to the increased enzymatic activity of Nox under proatherogenic shear conditions (52). *Ex vivo* shear models have also been refined to study the effects of other important mechanical forces in the vascular environment *in vivo* in addition to shear stress (49, 113). To tease apart the effects of shear stress and circumferential cyclic stretch on oxidative stress and vascular wall remodeling, an *ex vivo* setup was used in which stretching force parallel to the vessel's length can be controlled in addition to flow dynamics. The authors show that although superoxide production and activity of wall-remodeling proteases are shear dependent, reduced cyclic stretch enhances these effects, especially within the vascular endothelium. Further, reduced stretch also abrogated SMC contractility (165, 166). The aforementioned studies demonstrate the promise of *ex vivo* organ culture techniques to dissect the complex interactions of mechanical stresses in the vascular environment *in vivo* such as shear and cyclic stretch, and piece together their contributions toward oxidative stress and atherosclerosis.

Perspectives

Here, we reviewed *in vivo*, *in vitro*, and *ex vivo* models that have been used to study the relationship of shear stress, endothelial biology, and vascular diseases such as atherosclerosis. As for *in vitro* models, two of the most widely used and best characterized are the cone-and-plate and parallel-plate shear devices. These systems and modified versions have been critical in understanding molecular insights by which shear stress regulates endothelial function and structure under simple conditions.

Ex vivo culture models of shear stress attempt to combine the best of both worlds from *in vivo* and *in vitro* systems. Although retaining the advantage of controlling experimental conditions such as shear stress, *ex vivo* studies can be carried out without the confounding drawback of having to work with cultured cells, which can often behave very differently from somatic cells *in vivo*. In addition, they can also maintain vascular cells in their native tissue environment, that, while sacrificing experimental simplicity, adds more biological realism to *ex vivo* models. These *ex vivo* models can be carried out under *in vivo*-like mechanical conditions, including pulsatile flow, cyclic stretch, and oscillatory or LS together in one package.

Although *in vitro* and *ex vivo* models have their respective merits in simplifying the model such that specific mechanisms can be studied with more clarity and ease, animal models are still required to test most hypotheses addressed by *in vitro* and *ex vivo* models. However, the complexity of animal models and the differences between species may make the conclusions derived from animal models difficult to interpret. It is therefore of paramount importance to realize the constraints of various animal models and to choose the most relevant model for a particular study. It is also critical to compare the results obtained from *in vivo* models that acutely induce flow changes to that of endogenous flow-disturbed (atheroprone) or stable flow (atheroprotected) regions such as lesser curvature of the aortic arch and the thoracic aorta, respectively.

Shear stress intimately controls production of both NO and ROS levels in ECs by regulating both enzymes that produce these vasoactive factors as well as those that remove them. By controlling the redox balance in ECs, shear stress plays a critical role in regulating vascular biology and diseases such as inflammation and atherosclerosis. We believe that the combined use of *in vitro*, *ex vivo*, and *in vivo* models described here will provide crucial experimental systems to define the role of oxidative stress and signaling in flow-mediated vascular biology diseases.

Acknowledgments

H.J.'s work was supported by funding from NIH grants HL87012 (H.J.), HL75209 (H.J.), and UO1HL80711 (H.J.) and a

World Class University Project (H.J.) from the Ministry of Science, Technology, and Education of South Korea.

References

1. Adamo L, Naveiras O, Wenzel PL, McKinney-Freeman S, Mack PJ, Gracia-Sancho J, Suchy-Dicey A, Yoshimoto M, Lensch MW, Yoder MC, Garcia-Cardena G, and Daley GQ. Biomechanical forces promote embryonic haematopoiesis. *Nature* 459: 1131–1135, 2009.
2. Armstrong ML and Heistad DD. Animal models of atherosclerosis. *Atherosclerosis* 85: 15–23, 1990.
3. Asakura T and Karino T. Flow patterns and spatial distribution of atherosclerotic lesions in human coronary arteries. *Circ Res* 66: 1045–1066, 1990.
4. Bao X, Lu C, and Frangos JA. Temporal gradient in shear but not steady shear stress induces PDGF-A and MCP-1 expression in endothelial cells: role of NO, NF kappa B, and egr-1. *Arterioscler Thromb Vasc Biol* 19: 996–1003, 1999.
5. Bardy N, Karillon GJ, Merval R, Samuel JL, and Tedgui A. Differential effects of pressure and flow on DNA and protein synthesis and on fibronectin expression by arteries in a novel organ culture system. *Circ Res* 77: 684–694, 1995.
6. Barry-Lane PA, Patterson C, van der Merwe M, Hu Z, Holland SM, Yeh ET, and Runge MS. p47phox is required for atherosclerotic lesion progression in ApoE(−/−) mice. *J Clin Invest* 108: 1513–1522, 2001.
7. Birukov KG. Cyclic stretch, reactive oxygen species and vascular remodeling. *Antioxid Redox Signal* 11: 1651–1667, 2009.
8. Blackman BR, Barbee KA, and Thibault LE. *In vitro* cell shearing device to investigate the dynamic response of cells in a controlled hydrodynamic environment. *Ann Biomed Eng* 28: 363–372, 2000.
9. Blackman BR, Garcia-Cardena G, and Gimbrone MA, Jr. A new *in vitro* model to evaluate differential responses of endothelial cells to simulated arterial shear stress waveforms. *J Biomech Eng* 124: 397–407, 2002.
10. Booth RF, Martin JF, Honey AC, Hassall DG, Beesley JE, and Moncada S. Rapid development of atherosclerotic lesions in the rabbit carotid artery induced by perivascular manipulation. *Atherosclerosis* 76: 257–268, 1989.
11. Brooks AR, Lelkes PI, and Rubanyi GM. Gene expression profiling of human aortic endothelial cells exposed to disturbed flow and steady laminar flow. *Physiol Genomics* 9: 27–41, 2002.
12. Brown DC and Larson RS. Improvements to parallel plate flow chambers to reduce reagent and cellular requirements. *BMC Immunol* 2: 9, 2001.
13. Buchanan JR, Jr., Kleinstreuer C, Truskey GA, and Lei M. Relation between non-uniform hemodynamics and sites of altered permeability and lesion growth at the rabbit aortoceliac junction. *Atherosclerosis* 143: 27–40, 1999.
14. Bussolari SR, Dewey CF, Jr., and Gimbrone MA, Jr. Apparatus for subjecting living cells to fluid shear stress. *Rev Sci Instrum* 53: 1851–1854, 1982.
15. Carmeliet P, Moons L, Stassen JM, De Mol M, Bouche A, van den Oord JJ, Kockx M, and Collen D. Vascular wound healing and neointima formation induced by perivascular electric injury in mice. *Am J Pathol* 150: 761–776, 1997.
16. Caro CG. Discovery of the role of wall shear in atherosclerosis. *Arterioscler Thromb Vasc Biol* 29: 158–161, 2009.
17. Caro CG, Fitz-Gerald JM, and Schroter RC. Arterial wall shear and distribution of early atheroma in man. *Nature* 223: 1159–1160, 1969.
18. Caro CG, Fitz-Gerald JM, and Schroter RC. Atheroma and arterial wall shear. Observation, correlation and proposal of a shear dependent mass transfer mechanism for atherogenesis. *Proc R Soc Lond B Biol Sci* 177: 109–159, 1971.
19. Castier Y, Brandes RP, Leseche G, Tedgui A, and Lehoux S. p47phox-dependent NADPH oxidase regulates flow-induced vascular remodeling. *Circ Res* 97: 533–540, 2005.
20. Chakravarty S and Sen S. Analysis of pulsatile blood flow in constricted bifurcated arteries with vorticity-stream function approach. *J Med Eng Technol* 32: 10–22, 2008.
21. Chang K, Weiss D, Suo J, Vega JD, Giddens D, Taylor WR, and Jo H. Bone morphogenetic protein antagonists are coexpressed with bone morphogenetic protein 4 in endothelial cells exposed to unstable flow *in vitro* in mouse aortas and in human coronary arteries: role of bone morphogenetic protein antagonists in inflammation and atherosclerosis. *Circulation* 116: 1258–1266, 2007.
22. Cheng C, Helderman F, Tempel D, Segers D, Hierck B, Poelmann R, van Tol A, Duncker DJ, Robbers-Visser D, Ursem NT, van Haperen R, Wentzel JJ, Gijsen F, van der Steen AF, de Crom R, and Krams R. Large variations in absolute wall shear stress levels within one species and between species. *Atherosclerosis* 195: 225–235, 2007.
23. Cheng C, Tempel D, van Haperen R, de Boer HC, Segers D, Huisman M, van Zonneveld AJ, Leenen PJ, van der Steen A, Serruys PW, de Crom R, and Krams R. Shear stress-induced changes in atherosclerotic plaque composition are modulated by chemokines. *J Clin Invest* 117: 616–626, 2007.
24. Cheng C, Tempel D, van Haperen R, van der Baan A, Grosveld F, Daemen MJ, Krams R, and de Crom R. Atherosclerotic lesion size and vulnerability are determined by patterns of fluid shear stress. *Circulation* 113: 2744–2753, 2006.
25. Cheng C, van Haperen R, de Waard M, van Damme LC, Tempel D, Hanemaaijer L, van Cappellen GW, Bos J, Slager CJ, Duncker DJ, van der Steen AF, de Crom R, and Krams R. Shear stress affects the intracellular distribution of eNOS: direct demonstration by a novel *in vivo* technique. *Blood* 106: 3691–3698, 2005.
26. Cheng CP, Parker D, and Taylor CA. Quantification of wall shear stress in large blood vessels using Lagrangian interpolation functions with cine phase-contrast magnetic resonance imaging. *Ann Biomed Eng* 30: 1020–1032, 2002.
27. Chiu JJ, Chen LJ, Lee PL, Lee CI, Lo LW, Usami S, and Chien S. Shear stress inhibits adhesion molecule expression in vascular endothelial cells induced by coculture with smooth muscle cells. *Blood* 101: 2667–2674, 2003.
28. Chiu JJ, Usami S, and Chien S. Vascular endothelial responses to altered shear stress: pathologic implications for atherosclerosis. *Ann Med* 41: 19–28, 2009.
29. Civelek M, Manduchi E, Riley RJ, Stoeckert CJ, Jr., and Davies PF. Chronic endoplasmic reticulum stress activates unfolded protein response in arterial endothelium in regions of susceptibility to atherosclerosis. *Circ Res* 105: 453–461, 2009.

30. Clowes AW, Ryan GB, Breslow JL, and Karnovsky MJ. Absence of enhanced intimal thickening in the response of the carotid arterial wall to endothelial injury in hypercholesterolemic rats. *Lab Invest* 35: 6–17, 1976.
31. da Cunha V, Martin-McNulty B, Vincelette J, Choy DF, Li WW, Schroeder M, Mahmoudi M, Halks-Miller M, Wilson DW, Vergona R, Sullivan ME, and Wang YX. Angiotensin II induces histomorphologic features of unstable plaque in a murine model of accelerated atherosclerosis. *J Vasc Surg* 44: 364–371, 2006.
32. Dai G, Kaazempur-Mofrad MR, Natarajan S, Zhang Y, Vaughn S, Blackman BR, Kamm RD, Garcia-Cardena G, and Gimbrone MA, Jr. Distinct endothelial phenotypes evoked by arterial waveforms derived from atherosclerosis-susceptible and -resistant regions of human vasculature. *Proc Natl Acad Sci U S A* 101: 14871–14876, 2004.
33. Davies PF. Hemodynamic shear stress and the endothelium in cardiovascular pathophysiology. *Nat Clin Pract Cardiovasc Med* 6: 16–26, 2009.
34. Davies PF, Remuzzi A, Gordon EJ, Dewey CF, Jr., and Gimbrone MA, Jr. Turbulent fluid shear stress induces vascular endothelial cell turnover *in vitro*. *Proc Natl Acad Sci U S A* 83: 2114–2117, 1986.
35. Del Gaudio C, Morbiducci U, and Grigioni M. Time dependent non-Newtonian numerical study of the flow field in a realistic model of aortic arch. *Int J Artif Organs* 29: 709–718, 2006.
36. Dewey CF, Jr., Bussolari SR, Gimbrone MA, Jr., and Davies PF. The dynamic response of vascular endothelial cells to fluid shear stress. *J Biomech Eng* 103: 177–185, 1981.
37. Duguid JB and Robertson WB. Mechanical factors in atherosclerosis. *Lancet* 272: 1205–1209, 1957.
38. Eefting D, Bot I, de Vries MR, Schepers A, van Bockel JH, Van Berkel TJ, Biessen EA, and Quax PH. Local lentiviral short hairpin RNA silencing of CCR2 inhibits vein graft thickening in hypercholesterolemic apolipoprotein E3-Leiden mice. *J Vasc Surg* 50: 152–160, 2009.
39. Emanueli C, Salis MB, Chao J, Chao L, Agata J, Lin KF, Munao A, Straino S, Minasi A, Capogrossi MC, and Madeddu P. Adenovirus-mediated human tissue kallikrein gene delivery inhibits neointima formation induced by interruption of blood flow in mice. *Arterioscler Thromb Vasc Biol* 20: 1459–1466, 2000.
40. Faria-Neto JR, Chyu KY, Li X, Dimayuga PC, Ferreira C, Yano J, Cercek B, and Shah PK. Passive immunization with monoclonal IgM antibodies against phosphorylcholine reduces accelerated vein graft atherosclerosis in apolipoprotein E-null mice. *Atherosclerosis* 189: 83–90, 2006.
41. Farmakis TM, Soulis JV, Giannoglou GD, Zioupos GJ, and Louridas GE. Wall shear stress gradient topography in the normal left coronary arterial tree: possible implications for atherogenesis. *Curr Med Res Opin* 20: 587–596, 2004.
42. Feuerstein GZ and Ruffolo RR, Jr. Carvedilol, a novel vasodilating beta-blocker with the potential for cardiovascular organ protection. *Eur Heart J* 17 Suppl B: 24–29, 1996.
43. Fox JA and Hugh AE. Localization of atheroma: a theory based on boundary layer separation. *Br Heart J* 28: 388–399, 1966.
44. Frangos JA, Eskin SG, McIntire LV, and Ives CL. Flow effects on prostacyclin production by cultured human endothelial cells. *Science* 227: 1477–1479, 1985.
45. Frangos JA, McIntire LV, and Eskin SG. Shear stress induced stimulation of mammalian cell metabolism. *Biotechnol Bioeng* 32: 1053–1060, 1988.
46. Franke RP, Grafe M, Schnittler H, Seiffge D, Mittermayer C, and Drenckhahn D. Induction of human vascular endothelial stress fibres by fluid shear stress. *Nature* 307: 648–649, 1984.
47. Fry DL. Acute vascular endothelial changes associated with increased blood velocity gradients. *Circ Res* 22: 165–197, 1968.
48. Gambillara V, Chambaz C, Montorzi G, Roy S, Stergiopulos N, and Silacci P. Plaque-prone hemodynamics impair endothelial function in pig carotid arteries. *Am J Physiol Heart Circ Physiol* 290: H2320–H2328, 2006.
49. Gambillara V, Thacher T, Silacci P, and Stergiopulos N. Effects of reduced cyclic stretch on vascular smooth muscle cell function of pig carotids perfused *ex vivo*. *Am J Hypertens* 21: 425–431, 2008.
50. Girerd X, London G, Boutouyrie P, Mourad JJ, Safar M, and Laurent S. Remodeling of the radial artery in response to a chronic increase in shear stress. *Hypertension* 27: 799–803, 1996.
51. Go YM, Boo YC, Park H, Maland MC, Patel R, Pritchard KA, Jr., Fujio Y, Walsh K, Darley-Usmar V, and Jo H. Protein kinase B/Akt activates c-Jun NH(2)-terminal kinase by increasing NO production in response to shear stress. *J Appl Physiol* 91: 1574–1581, 2001.
52. Godbole AS, Lu X, Guo X, and Kassab GS. NADPH oxidase has a directional response to shear stress. *Am J Physiol Heart Circ Physiol* 296: H152–H158, 2009.
53. Godin D, Ivan E, Johnson C, Magid R, and Galis ZS. Remodeling of carotid artery is associated with increased expression of matrix metalloproteinases in mouse blood flow cessation model. *Circulation* 102: 2861–2866, 2000.
54. Gutierrez E, Petrich BG, Shattil SJ, Ginsberg MH, Groisman A, and Kasirer-Friede A. Microfluidic devices for studies of shear-dependent platelet adhesion. *Lab Chip* 8: 1486–1495, 2008.
55. Gutstein WH and Schneck DJ. *In vitro* boundary layer studies of blood flow in branched tubes. *J Atheroscler Res* 7: 295–299, 1967.
56. Guyton JR and Hartley CJ. Flow restriction of one carotid artery in juvenile rats inhibits growth of arterial diameter. *Am J Physiol* 248: H540–H546, 1985.
57. Haidekker MA, White CR, and Frangos JA. Analysis of temporal shear stress gradients during the onset phase of flow over a backward-facing step. *J Biomech Eng* 123: 455–463, 2001.
58. Hanyu M, Kume N, Ikeda T, Minami M, Kita T, and Komeda M. VCAM-1 expression precedes macrophage infiltration into subendothelium of vein grafts interposed into carotid arteries in hypercholesterolemic rabbits—a potential role in vein graft atherosclerosis. *Atherosclerosis* 158: 313–319, 2001.
59. Hardin NJ, Minick CR, and Murphy GE. Experimental induction of atheroarteriosclerosis by the synergy of allergic injury to arteries and lipid-rich diet. 3. The role of earlier acquired fibromuscular intimal thickening in the pathogenesis of later developing atherosclerosis. *Am J Pathol* 73: 301–326, 1973.
60. Helmlinger G, Geiger RV, Schreck S, and Nerem RM. Effects of pulsatile flow on cultured vascular endothelial cell morphology. *J Biomech Eng* 113: 123–131, 1991.
61. Hollestelle SC, De Vries MR, Van Keulen JK, Schoneveld AH, Vink A, Strijder CF, Van Middelaar BJ, Pasterkamp G, Quax PH, and De Kleijn DP. Toll-like receptor 4 is involved in outward arterial remodeling. *Circulation* 109: 393–398, 2004.

62. Hsiai TK, Cho SK, Honda HM, Hama S, Navab M, Demer LL, and Ho CM. Endothelial cell dynamics under pulsating flows: significance of high versus low shear stress slew rates (d(tau)/dt). *Ann Biomed Eng* 30: 646–656, 2002.
63. Hu Y, Zou Y, Dietrich H, Wick G, and Xu Q. Inhibition of neointima hyperplasia of mouse vein grafts by locally applied suramin. *Circulation* 100: 861–868, 1999.
64. Hugh AE and Fox JA. The precise localisation of atheroma and its association with stasis at the origin of the internal carotid artery—a radiographic investigation. *Br J Radiol* 43: 377–383, 1970.
65. Huo Y, Guo X, and Kassab GS. The flow field along the entire length of mouse aorta and primary branches. *Ann Biomed Eng* 36: 685–699, 2008.
66. Huo Y, Wischgoll T, and Kassab GS. Flow patterns in three-dimensional porcine epicardial coronary arterial tree. *Am J Physiol Heart Circ Physiol* 293: H2959–H2970, 2007.
67. Hwang J, Saha A, Boo YC, Sorescu GP, McNally JS, Holland SM, Dikalov S, Giddens DP, Griendling KK, Harrison DG, and Jo H. Oscillatory shear stress stimulates endothelial production of O2- from p47phox-dependent NAD(P)H oxidases, leading to monocyte adhesion. *J Biol Chem* 278: 47291–47298, 2003.
68. Ibrahim J, Miyashiro JK, and Berk BC. Shear stress is differentially regulated among inbred rat strains. *Circ Res* 92: 1001–1009, 2003.
69. Ignatowski AI. Ueber die Wirkung der tierschen Einweisse auf der Aorta. *Virchows Arch Pathol Anat* 198: 248, 1909.
70. Ishibashi S, Goldstein JL, Brown MS, Herz J, and Burns DK. Massive xanthomatosis and atherosclerosis in cholesterol-fed low density lipoprotein receptor-negative mice. *J Clin Invest* 93: 1885–1893, 1994.
71. Ishii A, Vinuela F, Murayama Y, Yuki I, Nien YL, Yeh DT, and Vinters HV. Swine model of carotid artery atherosclerosis: experimental induction by surgical partial ligation and dietary hypercholesterolemia. *AJNR Am J Neuroradiol* 27: 1893–1899, 2006.
72. Ivan E, Khatri JJ, Johnson C, Magid R, Godin D, Nandi S, Lessner S, and Galis ZS. Expansive arterial remodeling is associated with increased neointimal macrophage foam cell content: the murine model of macrophage-rich carotid artery lesions. *Circulation* 105: 2686–2691, 2002.
73. Jo H, Dull RO, Hollis TM, and Tarbell JM. Endothelial albumin permeability is shear dependent, time dependent, and reversible. *Am J Physiol* 260: H1992–H1996, 1991.
74. Jo H, Song H, and Mowbray A. Role of NADPH oxidases in disturbed flow- and BMP4-induced inflammation and atherosclerosis. *Antioxid Redox Signal* 8: 1609–1619, 2006.
75. Jokinen MP, Clarkson TB, and Prichard RW. Animal models in atherosclerosis research. *Exp Mol Pathol* 42: 1–28, 1985.
76. Jongstra-Bilen J, Haidari M, Zhu SN, Chen M, Guha D, and Cybulsky MI. Low-grade chronic inflammation in regions of the normal mouse arterial intima predisposed to atherosclerosis. *J Exp Med* 203: 2073–2083, 2006.
77. Jonsson-Rylander AC, Nilsson T, Fritsche-Danielson R, Hammarstrom A, Behrendt M, Andersson JO, Lindgren K, Andersson AK, Wallbrandt P, Rosengren B, Brodin P, Thelin A, Westin A, Hurt-Camejo E, and Lee-Sogaard CH. Role of ADAMTS-1 in atherosclerosis: remodeling of carotid artery, immunohistochemistry, and proteolysis of versican. *Arterioscler Thromb Vasc Biol* 25: 180–185, 2005.
78. Judkins CP, Diep H, Broughton BR, Mast AE, Hooker EU, Miller AA, Selemidis S, Dusting GJ, Sobey CG, and Drummond GR. Direct evidence of a role for Nox2 in superoxide production, reduced nitric oxide bioavailability, and early atherosclerotic plaque formation in ApoE−/− mice. *Am J Physiol Heart Circ Physiol* 298: H24–H32, 2010.
79. Kamiya A and Togawa T. Adaptive regulation of wall shear stress to flow change in the canine carotid artery. *Am J Physiol* 239: H14–H21, 1980.
80. Kawashima S, Yamashita T, Ozaki M, Ohashi Y, Azumi H, Inoue N, Hirata K, Hayashi Y, Itoh H, and Yokoyama M. Endothelial NO synthase overexpression inhibits lesion formation in mouse model of vascular remodeling. *Arterioscler Thromb Vasc Biol* 21: 201–207, 2001.
81. Khatri JJ, Johnson C, Magid R, Lessner SM, Laude KM, Dikalov SI, Harrison DG, Sung HJ, Rong Y, and Galis ZS. Vascular oxidant stress enhances progression and angiogenesis of experimental atheroma. *Circulation* 109: 520–525, 2004.
82. Kikuchi S, Umemura K, Kondo K, Saniabadi AR, and Nakashima M. Photochemically induced endothelial injury in the mouse as a screening model for inhibitors of vascular intimal thickening. *Arterioscler Thromb Vasc Biol* 18: 1069–1078, 1998.
83. Kirk EA, Dinauer MC, Rosen H, Chait A, Heinecke JW, and LeBoeuf RC. Impaired superoxide production due to a deficiency in phagocyte NADPH oxidase fails to inhibit atherosclerosis in mice. *Arterioscler Thromb Vasc Biol* 20: 1529–1535, 2000.
84. Kleinstreuer C, Hyun S, Buchanan JR, Jr., Longest PW, Archie JP, Jr., and Truskey GA. Hemodynamic parameters and early intimal thickening in branching blood vessels. *Crit Rev Biomed Eng* 29: 1–64, 2001.
85. Korshunov VA and Berk BC. Flow-induced vascular remodeling in the mouse: a model for carotid intima-media thickening. *Arterioscler Thromb Vasc Biol* 23: 2185–2191, 2003.
86. Korshunov VA and Berk BC. Strain-dependent vascular remodeling: the "Glagov phenomenon" is genetically determined. *Circulation* 110: 220–226, 2004.
87. Koslow AR, Stromberg RR, Friedman LI, Lutz RJ, Hilbert SL, and Schuster P. A flow system for the study of shear forces upon cultured endothelial cells. *J Biomech Eng* 108: 338–341, 1986.
88. Kotha J, Zhang C, Longhurst CM, Lu Y, Jacobs J, Cheng Y, and Jennings LK. Functional relevance of tetraspanin CD9 in vascular smooth muscle cell injury phenotypes: a novel target for the prevention of neointimal hyperplasia. *Atherosclerosis* 203: 377–386, 2009.
89. Ku DN, Giddens DP, Zarins CK, and Glagov S. Pulsatile flow and atherosclerosis in the human carotid bifurcation. Positive correlation between plaque location and low oscillating shear stress. *Arteriosclerosis* 5: 293–302, 1985.
90. Langille BL and O'Donnell F. Reductions in arterial diameter produced by chronic decreases in blood flow are endothelium-dependent. *Science* 231: 405–407, 1986.
91. Lardenoye JH, Delsing DJ, de Vries MR, Deckers MM, Princen HM, Havekes LM, van Hinsbergh VW, van Bockel JH, and Quax PH. Accelerated atherosclerosis by placement of a perivascular cuff and a cholesterol-rich diet in ApoE*3Leiden transgenic mice. *Circ Res* 87: 248–253, 2000.
92. Lawrence MB, McIntire LV, and Eskin SG. Effect of flow on polymorphonuclear leukocyte/endothelial cell adhesion. *Blood* 70: 1284–1290, 1987.
93. Lei M, Kleinstreuer C, and Truskey GA. Numerical investigation and prediction of atherogenic sites in branching arteries. *J Biomech Eng* 117: 350–357, 1995.

94. Leidenfrost JE, Khan MF, Boc KP, Villa BR, Collins ET, Parks WC, Abendschein DR, and Choi ET. A model of primary atherosclerosis and post-angioplasty restenosis in mice. *Am J Pathol* 163: 773–778, 2003.
95. Levesque MJ, Liepsch D, Moravec S, and Nerem RM. Correlation of endothelial cell shape and wall shear stress in a stenosed dog aorta. *Arteriosclerosis* 6: 220–229, 1986.
96. Levesque MJ and Nerem RM. The elongation and orientation of cultured endothelial cells in response to shear stress. *J Biomech Eng* 107: 341–347, 1985.
97. Li L, Rezvan A, Salerno JC, Husain A, Kwon K, Jo H, Harrison DG, and Chen W. GTP cyclohydrolase I phosphorylation and interaction with GTP cyclohydrolase feedback regulatory protein provide novel regulation of endothelial tetrahydrobiopterin and nitric oxide. *Circ Res* 106: 328–336, 2010.
98. Li X, Chyu KY, Faria Neto JR, Yano J, Nathwani N, Ferreira C, Dimayuga PC, Cercek B, Kaul S, and Shah PK. Differential effects of apolipoprotein A-I-mimetic peptide on evolving and established atherosclerosis in apolipoprotein E-null mice. *Circulation* 110: 1701–1705, 2004.
99. Liang C, Xiaonan L, Xiaojun C, Changjiang L, Xinsheng X, Guihua J, Xiaobo H, Yanen Z, Runyi S, Huixia L, Yun Z, and Mei Z. Effect of metoprolol on vulnerable plaque in rabbits by changing shear stress around plaque and reducing inflammation. *Eur J Pharmacol* 613: 79–85, 2009.
100. Lichtman AH, Clinton SK, Iiyama K, Connelly PW, Libby P, and Cybulsky MI. Hyperlipidemia and atherosclerotic lesion development in LDL receptor-deficient mice fed defined semipurified diets with and without cholate. *Arterioscler Thromb Vasc Biol* 19: 1938–1944, 1999.
101. Lindner V, Fingerle J, and Reidy MA. Mouse model of arterial injury. *Circ Res* 73: 792–796, 1993.
102. Liu SL, Li YH, Shi GY, Tang SH, Jiang SJ, Huang CW, Liu PY, Hong JS, and Wu HL. Dextromethorphan reduces oxidative stress and inhibits atherosclerosis and neointima formation in mice. *Cardiovasc Res* 82: 161–169, 2009.
103. Loke WM, Proudfoot JM, Hodgson JM, McKinley AJ, Hime N, Magat M, Stocker R, and Croft KD. Specific dietary polyphenols attenuate atherosclerosis in apolipoprotein e-knockout mice by alleviating inflammation and endothelial dysfunction. *Arterioscler Thromb Vasc Biol* 30: 749–757, 2010.
104. Lu X and Kassab GS. Nitric oxide is significantly reduced in *ex vivo* porcine arteries during reverse flow because of increased superoxide production. *J Physiol* 561: 575–582, 2004.
105. Lukowski R, Weinmeister P, Bernhard D, Feil S, Gotthardt M, Herz J, Massberg S, Zernecke A, Weber C, Hofmann F, and Feil R. Role of smooth muscle cGMP/cGKI signaling in murine vascular restenosis. *Arterioscler Thromb Vasc Biol* 28: 1244–1250, 2008.
106. Lutz RJ, Cannon JN, Bischoff KB, Dedrick RL, Stiles RK, and Fry DL. Wall shear stress distribution in a model canine artery during steady flow. *Circ Res* 41: 391–399, 1977.
107. Malek AM, Alper SL, and Izumo S. Hemodynamic shear stress and its role in atherosclerosis. *JAMA* 282: 2035–2042, 1999.
108. McPherson JA, Barringhaus KG, Bishop GG, Sanders JM, Rieger JM, Hesselbacher SE, Gimple LW, Powers ER, Macdonald T, Sullivan G, Linden J, and Sarembock IJ. Adenosine A(2A) receptor stimulation reduces inflammation and neointimal growth in a murine carotid ligation model. *Arterioscler Thromb Vasc Biol* 21: 791–796, 2001.
109. Melkumyants AM, Balashov SA, and Khayutin VM. Endothelium dependent control of arterial diameter by blood viscosity. *Cardiovasc Res* 23: 741–747, 1989.
110. Minick CR and Murphy GE. Experimental induction of atheroarteriosclerosis by the synergy of allergic injury to arteries and lipid-rich diet. II. Effect of repeatedly injected foreign protein in rabbits fed a lipid-rich, cholesterol-poor diet. *Am J Pathol* 73: 265–300, 1973.
111. Miyashiro JK, Poppa V, and Berk BC. Flow-induced vascular remodeling in the rat carotid artery diminishes with age. *Circ Res* 81: 311–319, 1997.
112. Mondy JS, Lindner V, Miyashiro JK, Berk BC, Dean RH, and Geary RL. Platelet-derived growth factor ligand and receptor expression in response to altered blood flow *in vivo*. *Circ Res* 81: 320–327, 1997.
113. Montorzi G, Silacci P, Zulliger M, and Stergiopulos N. Functional, mechanical and geometrical adaptation of the arterial wall of a non-axisymmetric artery *in vitro*. *J Hypertens* 22: 339–347, 2004.
114. Moore JE, Jr., Burki E, Suciu A, Zhao S, Burnier M, Brunner HR, and Meister JJ. A device for subjecting vascular endothelial cells to both fluid shear stress and circumferential cyclic stretch. *Ann Biomed Eng* 22: 416–422, 1994.
115. Morishita T, Tsutsui M, Shimokawa H, Horiuchi M, Tanimoto A, Suda O, Tasaki H, Huang PL, Sasaguri Y, Yanagihara N, and Nakashima Y. Vasculoprotective roles of neuronal nitric oxide synthase. *FASEB J* 16: 1994–1996, 2002.
116. Mowbray AL, Kang DH, Rhee SG, Kang SW, and Jo H. Laminar shear stress up-regulates peroxiredoxins (PRX) in endothelial cells: PRX 1 as a mechanosensitive antioxidant. *J Biol Chem* 283: 1622–1627, 2008.
117. Mukai Y, Rikitake Y, Shiojima I, Wolfrum S, Satoh M, Takeshita K, Hiroi Y, Salomone S, Kim HH, Benjamin LE, Walsh K, and Liao JK. Decreased vascular lesion formation in mice with inducible endothelial-specific expression of protein kinase Akt. *J Clin Invest* 116: 334–343, 2006.
118. Nackman GB, Fillinger MF, Shafritz R, Wei T, and Graham AM. Flow modulates endothelial regulation of smooth muscle cell proliferation: a new model. *Surgery* 124: 353–360; discussion 360–351, 1998.
119. Nagel T, Resnick N, Dewey CF, Jr., and Gimbrone MA, Jr. Vascular endothelial cells respond to spatial gradients in fluid shear stress by enhanced activation of transcription factors. *Arterioscler Thromb Vasc Biol* 19: 1825–1834, 1999.
120. Nakamura K, Sasaki T, Cheng XW, Iguchi A, Sato K, and Kuzuya M. Statin prevents plaque disruption in apoE-knockout mouse model through pleiotropic effect on acute inflammation. *Atherosclerosis* 206: 355–361, 2009.
121. Nam D, Ni CW, Rezvan A, Suo J, Budzyn K, Llanos A, Harrison D, Giddens D, and Jo H. Partial carotid ligation is a model of acutely induced disturbed flow, leading to rapid endothelial dysfunction and atherosclerosis. *Am J Physiol Heart Circ Physiol* 297: H1535–H1543, 2009.
122. Ojha M. Wall shear stress temporal gradient and anastomotic intimal hyperplasia. *Circ Res* 74: 1227–1231, 1994.
123. Paigen B, Mitchell D, Reue K, Morrow A, Lusis AJ, and LeBoeuf RC. Ath-1, a gene determining atherosclerosis susceptibility and high density lipoprotein levels in mice. *Proc Natl Acad Sci U S A* 84: 3763–3767, 1987.
124. Paigen B, Morrow A, Brandon C, Mitchell D, and Holmes P. Variation in susceptibility to atherosclerosis among inbred strains of mice. *Atherosclerosis* 57: 65–73, 1985.

125. Paulson KE, Zhu SN, Chen M, Nurmohamed S, Jongstra-Bilen J, and Cybulsky MI. Resident intimal dendritic cells accumulate lipid and contribute to the initiation of atherosclerosis. *Circ Res* 106: 383–390, 2010.
126. Pearce JD, Li J, Edwards MS, English WP, and Geary RL. Differential effects of Rho-kinase inhibition on artery wall mass and remodeling. *J Vasc Surg* 39: 223–228, 2004.
127. Piedrahita JA, Zhang SH, Hagaman JR, Oliver PM, and Maeda N. Generation of mice carrying a mutant apolipoprotein E gene inactivated by gene targeting in embryonic stem cells. *Proc Natl Acad Sci U S A* 89: 4471–4475, 1992.
128. Platt MO, Ankeny RF, and Jo H. Laminar shear stress inhibits cathepsin L activity in endothelial cells. *Arterioscler Thromb Vasc Biol* 26: 1784–1790, 2006.
129. Platt MO, Ankeny RF, Shi GP, Weiss D, Vega JD, Taylor WR, and Jo H. Expression of cathepsin K is regulated by shear stress in cultured endothelial cells and is increased in endothelium in human atherosclerosis. *Am J Physiol Heart Circ Physiol* 292: H1479–H1486, 2007.
130. Plump AS, Smith JD, Hayek T, Aalto-Setala K, Walsh A, Verstuyft JG, Rubin EM, and Breslow JL. Severe hypercholesterolemia and atherosclerosis in apolipoprotein E-deficient mice created by homologous recombination in ES cells. *Cell* 71: 343–353, 1992.
131. Prado CM, Ramos SG, Alves-Filho JC, Elias J, Jr., Cunha FQ, and Rossi MA. Turbulent flow/low wall shear stress and stretch differentially affect aorta remodeling in rats. *J Hypertens* 24: 503–515, 2006.
132. Prado CM, Ramos SG, Elias J, Jr., and Rossi MA. Turbulent blood flow plays an essential localizing role in the development of atherosclerotic lesions in experimentally induced hypercholesterolaemia in rats. *Int J Exp Pathol* 89: 72–80, 2008.
133. Qiao AK, Guo XL, Wu SG, Zeng YJ, and Xu XH. Numerical study of nonlinear pulsatile flow in S-shaped curved arteries. *Med Eng Phys* 26: 545–552, 2004.
134. Qin F, Impeduglia T, Schaffer P, and Dardik H. Overexpression of von Willebrand factor is an independent risk factor for pathogenesis of intimal hyperplasia: preliminary studies. *J Vasc Surg* 37: 433–439, 2003.
135. Qiu Y and Tarbell JM. Interaction between wall shear stress and circumferential strain affects endothelial cell biochemical production. *J Vasc Res* 37: 147–157, 2000.
136. Qiu Y and Tarbell JM. Numerical simulation of pulsatile flow in a compliant curved tube model of a coronary artery. *J Biomech Eng* 122: 77–85, 2000.
137. Rainger GE, Stone P, Morland CM, and Nash GB. A novel system for investigating the ability of smooth muscle cells and fibroblasts to regulate adhesion of flowing leukocytes to endothelial cells. *J Immunol Methods* 255: 73–82, 2001.
138. Rectenwald JE, Minter RM, Moldawer LL, Abouhamze Z, La Face D, Hutchins E, Huber TS, Seeger JM, and Ozaki CK. Interleukin-10 fails to modulate low shear stress-induced neointimal hyperplasia. *J Surg Res* 102: 110–118, 2002.
139. Rekhter M, Staschke K, Estridge T, Rutherford P, Jackson N, Gifford-Moore D, Foxworthy P, Reidy C, Huang XD, Kalbfleisch M, Hui K, Kuo MS, Gilmour R, and Vlahos CJ. Genetic ablation of IRAK4 kinase activity inhibits vascular lesion formation. *Biochem Biophys Res Commun* 367: 642–648, 2008.
140. Resnick N and Gimbrone MA, Jr. Hemodynamic forces are complex regulators of endothelial gene expression. *FASEB J* 9: 874–882, 1995.
141. Rudic RD, Bucci M, Fulton D, Segal SS, and Sessa WC. Temporal events underlying arterial remodeling after chronic flow reduction in mice: correlation of structural changes with a deficit in basal nitric oxide synthesis. *Circ Res* 86: 1160–1166, 2000.
142. Rudic RD, Shesely EG, Maeda N, Smithies O, Segal SS, and Sessa WC. Direct evidence for the importance of endothelium-derived nitric oxide in vascular remodeling. *J Clin Invest* 101: 731–736, 1998.
143. Sabiston DC, Jr., Smith GW, Talbert JL, Gutelius J, and Vasko JS. Experimental production of canine coronary atherosclerosis. *Ann Surg* 153: 13–22, 1961.
144. Samet MM and Lelkes PI. Pulsatile flow and endothelial cell morphology in a cell culture chamber model of an artificial cardiac ventricle. *J Biomech Eng* 116: 369–371, 1994.
145. Sasaguri Y, Wang KY, Tanimoto A, Tsutsui M, Ueno H, Murata Y, Kohno Y, Yamada S, and Ohtsu H. Role of histamine produced by bone marrow-derived vascular cells in pathogenesis of atherosclerosis. *Circ Res* 96: 974–981, 2005.
146. Satoh K, Matoba T, Suzuki J, O'Dell MR, Nigro P, Cui Z, Mohan A, Pan S, Li L, Jin ZG, Yan C, Abe J, and Berk BC. Cyclophilin A mediates vascular remodeling by promoting inflammation and vascular smooth muscle cell proliferation. *Circulation* 117: 3088–3098, 2008.
147. Savage B, Saldivar E, and Ruggeri ZM. Initiation of platelet adhesion by arrest onto fibrinogen or translocation on von Willebrand factor. *Cell* 84: 289–297, 1996.
148. Sawchuk AP, Unthank JL, Davis TE, and Dalsing MC. A prospective, *in vivo* study of the relationship between blood flow hemodynamics and atherosclerosis in a hyperlipidemic swine model. *J Vasc Surg* 19: 58–63; discussion 63–54, 1994.
149. Schaff UY, Xing MM, Lin KK, Pan N, Jeon NL, and Simon SI. Vascular mimetics based on microfluidics for imaging the leukocyte—endothelial inflammatory response. *Lab Chip* 7: 448–456, 2007.
150. Schepers A, de Vries MR, van Leuven CJ, Grimbergen JM, Holers VM, Daha MR, van Bockel JH, and Quax PH. Inhibition of complement component C3 reduces vein graft atherosclerosis in apolipoprotein E3-Leiden transgenic mice. *Circulation* 114: 2831–2838, 2006.
151. Schnittler HJ, Franke RP, Akbay U, Mrowietz C, and Drenckhahn D. Improved *in vitro* rheological system for studying the effect of fluid shear stress on cultured cells. *Am J Physiol* 265: C289–C298, 1993.
152. Shao J, Wu L, Wu J, Zheng Y, Zhao H, Jin Q, and Zhao J. Integrated microfluidic chip for endothelial cells culture and analysis exposed to a pulsatile and oscillatory shear stress. *Lab Chip* 9: 3118–3125, 2009.
153. Shi ZS, Feng L, He X, Ishii A, Goldstine J, Vinters HV, and Vinuela F. Vulnerable plaque in a Swine model of carotid atherosclerosis. *AJNR Am J Neuroradiol* 30: 469–472, 2009.
154. Sill HW, Chang YS, Artman JR, Frangos JA, Hollis TM, and Tarbell JM. Shear stress increases hydraulic conductivity of cultured endothelial monolayers. *Am J Physiol* 268: H535–H543, 1995.
155. Simmers MB, Pryor AW, and Blackman BR. Arterial shear stress regulates endothelial cell-directed migration, polarity, and morphology in confluent monolayers. *Am J Physiol Heart Circ Physiol* 293: H1937–H1946, 2007.
156. Sindermann JR, Smith J, Kobbert C, Plenz G, Skaletz-Rorowski A, Solomon JL, Fan L, and March KL. Direct

evidence for the importance of p130 in injury response and arterial remodeling following carotid artery ligation. *Cardiovasc Res* 54: 676–683, 2002.
157. Sorescu GP, Song H, Tressel SL, Hwang J, Dikalov S, Smith DA, Boyd NL, Platt MO, Lassegue B, Griendling KK, and Jo H. Bone morphogenetic protein 4 produced in endothelial cells by oscillatory shear stress induces monocyte adhesion by stimulating reactive oxygen species production from a nox1-based NADPH oxidase. *Circ Res* 95: 773–779, 2004.
158. Sorescu GP, Sykes M, Weiss D, Platt MO, Saha A, Hwang J, Boyd N, Boo YC, Vega JD, Taylor WR, and Jo H. Bone morphogenetic protein 4 produced in endothelial cells by oscillatory shear stress stimulates an inflammatory response. *J Biol Chem* 278: 31128–31135, 2003.
159. Sullivan CJ and Hoying JB. Flow-dependent remodeling in the carotid artery of fibroblast growth factor-2 knockout mice. *Arterioscler Thromb Vasc Biol* 22: 1100–1105, 2002.
160. Sun N, Wood NB, Hughes AD, Thom SA, and Yun Xu X. Effects of transmural pressure and wall shear stress on LDL accumulation in the arterial wall: a numerical study using a multilayered model. *Am J Physiol Heart Circ Physiol* 292: H3148–H3157, 2007.
161. Suo J, Ferrara DE, Sorescu D, Guldberg RE, Taylor WR, and Giddens DP. Hemodynamic shear stresses in mouse aortas: implications for atherogenesis. *Arterioscler Thromb Vasc Biol* 27: 346–351, 2007.
162. Tang BT, Cheng CP, Draney MT, Wilson NM, Tsao PS, Herfkens RJ, and Taylor CA. Abdominal aortic hemodynamics in young healthy adults at rest and during lower limb exercise: quantification using image-based computer modeling. *Am J Physiol Heart Circ Physiol* 291: H668–H676, 2006.
163. Tang PC, Qin L, Zielonka J, Zhou J, Matte-Martone C, Bergaya S, van Rooijen N, Shlomchik WD, Min W, Sessa WC, Pober JS, and Tellides G. MyD88-dependent, superoxide-initiated inflammation is necessary for flow-mediated inward remodeling of conduit arteries. *J Exp Med* 205: 3159–3171, 2008.
164. Texon M. The hemodynamic concept of atherosclerosis. *Bull N Y Acad Med* 36: 263–274, 1960.
165. Thacher T, da Silva RF, and Stergiopulos N. Differential effects of reduced cyclic stretch and perturbed shear stress within the arterial wall and on smooth muscle function. *Am J Hypertens* 22: 1250–1257, 2009.
166. Thacher T, Gambillara V, da Silva RF, Silacci P, and Stergiopulos N. Reduced cyclic stretch, endothelial dysfunction, and oxidative stress: an *ex vivo* model. *Cardiovasc Pathol* 19:e91–e98, 2010.
167. Thomas WA and Hartroft WS. Myocardial infarction in rats fed diets containing high fat, cholesterol, thiouracil, and sodium cholate. *Circulation* 19: 65–72, 1959.
168. Thompson JS. Atheromata in an inbred strain of mice. *J Atheroscler Res* 10: 113–122, 1969.
169. Tkachenko E, Gutierrez E, Ginsberg MH, and Groisman A. An easy to assemble microfluidic perfusion device with a magnetic clamp. *Lab Chip* 9: 1085–1095, 2009.
170. Traub O and Berk BC. Laminar shear stress: mechanisms by which endothelial cells transduce an atheroprotective force. *Arterioscler Thromb Vasc Biol* 18: 677–685, 1998.
171. Tressel SL, Huang RP, Tomsen N, and Jo H. Laminar shear inhibits tubule formation and migration of endothelial cells by an angiopoietin-2 dependent mechanism. *Arterioscler Thromb Vasc Biol* 27: 2150–2156, 2007.
172. Truskey GA, Barber KM, Robey TC, Olivier LA, and Combs MP. Characterization of a sudden expansion flow chamber to study the response of endothelium to flow recirculation. *J Biomech Eng* 117: 203–210, 1995.
173. Tsou JK, Gower RM, Ting HJ, Schaff UY, Insana MF, Passerini AG, and Simon SI. Spatial regulation of inflammation by human aortic endothelial cells in a linear gradient of shear stress. *Microcirculation* 15: 311–323, 2008.
174. Tsutsui M. Neuronal nitric oxide synthase as a novel anti-atherogenic factor. *J Atheroscler Thromb* 11: 41–48, 2004.
175. Usami S, Chen HH, Zhao Y, Chien S, and Skalak R. Design and construction of a linear shear stress flow chamber. *Ann Biomed Eng* 21: 77–83, 1993.
176. von der Thusen JH, van Berkel TJ, and Biessen EA. Induction of rapid atherogenesis by perivascular carotid collar placement in apolipoprotein E-deficient and low-density lipoprotein receptor-deficient mice. *Circulation* 103: 1164–1170, 2001.
177. Wang N, Miao H, Li YS, Zhang P, Haga JH, Hu Y, Young A, Yuan S, Nguyen P, Wu CC, and Chien S. Shear stress regulation of Kruppel-like factor 2 expression is flow pattern-specific. *Biochem Biophys Res Commun* 341: 1244–1251, 2006.
178. Wang Y, Bai Y, Qin L, Zhang P, Yi T, Teesdale SA, Zhao L, Pober JS, and Tellides G. Interferon-gamma induces human vascular smooth muscle cell proliferation and intimal expansion by phosphatidylinositol 3-kinase dependent mammalian target of rapamycin raptor complex 1 activation. *Circ Res* 101: 560–569, 2007.
179. Warabi E, Wada Y, Kajiwara H, Kobayashi M, Koshiba N, Hisada T, Shibata M, Ando J, Tsuchiya M, Kodama T, and Noguchi N. Effect on endothelial cell gene expression of shear stress, oxygen concentration, and low-density lipoprotein as studied by a novel flow cell culture system. *Free Radic Biol Med* 37: 682–694, 2004.
180. White CR, Haidekker M, Bao X, and Frangos JA. Temporal gradients in shear, but not spatial gradients, stimulate endothelial cell proliferation. *Circulation* 103: 2508–2513, 2001.
181. Won D, Zhu SN, Chen M, Teichert AM, Fish JE, Matouk CC, Bonert M, Ojha M, Marsden PA, and Cybulsky MI. Relative reduction of endothelial nitric-oxide synthase expression and transcription in atherosclerosis-prone regions of the mouse aorta and in an *in vitro* model of disturbed flow. *Am J Pathol* 171: 1691–1704, 2007.
182. Xu Q. Mouse models of arteriosclerosis: from arterial injuries to vascular grafts. *Am J Pathol* 165: 1–10, 2004.
183. Yamada S, Wang KY, Tanimoto A, Fan J, Shimajiri S, Kitajima S, Morimoto M, Tsutsui M, Watanabe T, Yasumoto K, and Sasaguri Y. Matrix metalloproteinase 12 accelerates the initiation of atherosclerosis and stimulates the progression of fatty streaks to fibrous plaques in transgenic rabbits. *Am J Pathol* 172: 1419–1429, 2008.
184. Yamamoto Y, Ogino K, Igawa G, Matsuura T, Kaetsu Y, Sugihara S, Matsubara K, Miake J, Hamada T, Yoshida A, Igawa O, Yamamoto T, Shigemasa C, and Hisatome I. Allopurinol reduces neointimal hyperplasia in the carotid artery ligation model in spontaneously hypertensive rats. *Hypertens Res* 29: 915–921, 2006.
185. Yamashita T, Kawashima S, Ozaki M, Rikitake Y, Hirase T, Inoue N, Hirata K, and Yokoyama M. A calcium channel blocker, benidipine, inhibits intimal thickening in the carotid artery of mice by increasing nitric oxide production. *J Hypertens* 19: 451–458, 2001.

186. Yamawaki H, Lehoux S, and Berk BC. Chronic physiological shear stress inhibits tumor necrosis factor-induced proinflammatory responses in rabbit aorta perfused *ex vivo*. *Circulation* 108: 1619–1625, 2003.
187. Yogo K, Shimokawa H, Funakoshi H, Kandabashi T, Miyata K, Okamoto S, Egashira K, Huang P, Akaike T, and Takeshita A. Different vasculoprotective roles of NO synthase isoforms in vascular lesion formation in mice. *Arterioscler Thromb Vasc Biol* 20: E96–E100, 2000.
188. Zakaria H, Robertson AM, and Kerber CW. A parametric model for studies of flow in arterial bifurcations. *Ann Biomed Eng* 36: 1515–1530, 2008.
189. Zarins CK, Giddens DP, Bharadvaj BK, Sottiurai VS, Mabon RF, and Glagov S. Carotid bifurcation atherosclerosis. Quantitative correlation of plaque localization with flow velocity profiles and wall shear stress. *Circ Res* 53: 502–514, 1983.
190. Zarins CK, Zatina MA, Giddens DP, Ku DN, and Glagov S. Shear stress regulation of artery lumen diameter in experimental atherogenesis. *J Vasc Surg* 5: 413–420, 1987.
191. Zhang LN, Parkinson JF, Haskell C, and Wang YX. Mechanisms of intimal hyperplasia learned from a murine carotid artery ligation model. *Curr Vasc Pharmacol* 6: 37–43, 2008.
192. Zhang LN, Wilson DW, da Cunha V, Sullivan ME, Vergona R, Rutledge JC, and Wang YX. Endothelial NO synthase deficiency promotes smooth muscle progenitor cells in association with upregulation of stromal cell-derived factor-1alpha in a mouse model of carotid artery ligation. *Arterioscler Thromb Vasc Biol* 26: 765–772, 2006.
193. Zhang SH, Reddick RL, Piedrahita JA, and Maeda N. Spontaneous hypercholesterolemia and arterial lesions in mice lacking apolipoprotein E. *Science* 258: 468–471, 1992.
194. Zhu Y, Farrehi PM, and Fay WP. Plasminogen activator inhibitor type 1 enhances neointima formation after oxidative vascular injury in atherosclerosis-prone mice. *Circulation* 103: 3105–3110, 2001.
195. Zou Y, Dietrich H, Hu Y, Metzler B, Wick G, and Xu Q. Mouse model of venous bypass graft arteriosclerosis. *Am J Pathol* 153: 1301–1310, 1998.

Address correspondence to:
Prof. Hanjoong Jo
Coulter Department of Biomedical Engineering
Georgia Institute of Technology
Emory University
Woodruff Memorial Building 2005
Atlanta, GA 30322

E-mail: hjo@bme.gatech.edu

Date of first submission to ARS Central, July 22, 2010; date of acceptance, August 13, 2010.

Abbreviations Used

ApoE = apolipoprotein E
A/V = arterio-venous
BMP4 = bone morphogenetic protein 4
EC = endothelial cell
ECA = external carotid artery
eNOS = endothelial nitric oxide synthase
ICA = internal carotid artery
ICAM-1 = inter-cellular adhesion molecule 1
KO = knockout
LCA = left common carotid artery
LS = laminar shear
LSA = left subclavian artery
NO = nitric oxide
Nox = NADPH oxidase
OA = occipital artery
OS = oscillatory shear
PDMS = polydimethylsiloxane
RCA = right common carotid artery
ROS = reactive oxygen species
RSA = right subclavian artery
SMC = smooth muscle cell
SPA = stress phase angle
STA = superior thyroid artery
VCAM-1 = vascular cell adhesion molecule 1

This article has been cited by:

1. Dong Ju Son, Soo Yeon Kim, Seong Su Han, Chan Woo Kim, Sandeep Kumar, Byeoung Soo Park, Sung Eun Lee, Yeo Pyo Yun, Hanjoong Jo, Young Hyun Park. 2012. Piperlongumine inhibits atherosclerotic plaque formation and vascular smooth muscle cell proliferation by suppressing PDGF receptor signaling. *Biochemical and Biophysical Research Communications* . [CrossRef]
2. Noriko Noguchi , Hanjoong Jo . Redox Going with Vascular Shear Stress. *Antioxidants & Redox Signaling*, ahead of print. [Abstract] [Full Text HTML] [Full Text PDF] [Full Text PDF with Links]
3. Wakako Takabe , Eiji Warabi , Noriko Noguchi . Anti-Atherogenic Effect of Laminar Shear Stress via Nrf2 Activation. *Antioxidants & Redox Signaling*, ahead of print. [Abstract] [Full Text HTML] [Full Text PDF] [Full Text PDF with Links] [Supplemental material]
4. Patrizia Nigro , Jun-ichi Abe , Bradford C. Berk . Flow Shear Stress and Atherosclerosis: A Matter of Site Specificity. *Antioxidants & Redox Signaling*, ahead of print. [Abstract] [Full Text HTML] [Full Text PDF] [Full Text PDF with Links]